A thermal non-equilibrium model with Cattaneo effect for convection in a Brinkman porous layer

I. S. Shivakumara[a], M. Ravisha[b], Chiu-On Ng[c*], V. L. Varun[a]

[a]Department of Mathematics, Bangalore University, Bangalore 560 001, India

[b]Department of Mathematics, Dr. G. Shankar Government Women's First Grade College and Post Graduate Study Centre, Ajjarakadu, Udupi-576101, India

[c]Department of Mechanical Engineering, The University of Hong Kong, Pokfulam Road, Hong Kong, China

---

ABSTRACT

This paper aims to investigate the onset of thermal convection in a layer of fluid-saturated Brinkman porous medium taking into account fluid inertia and local thermal non-equilibrium (LTNE) between the solid and fluid phases with Cattaneo effect in the solid. A two-field model is used for the energy equations each representing the solid and fluid phases separately. The usual Fourier heat-transfer law is retained in the fluid phase while the solid phase is allowed to transfer heat via a Cattaneo heat flux theory. It is observed that the Cattaneo effect has a profound influence on the nature of convective instability. In contrast to the standard Brinkman convection with LTNE model, instability is found to occur through oscillatory convection depending on the value of solid thermal relaxation time parameter which in turn depends on other parametric values. The instability characteristics of the system are analyzed in detail for a wide range of parametric values including those for copper oxide and aluminium oxide solid skeletons.

Key words: Brinkman porous medium, Cattaneo effect, LTNE model, Thermal convection

---

***Corresponding author:** Chiu-On Ng, E-mail: cong@hku.hk

1. Introduction

Buoyancy driven convection in a horizontal porous layer subject to an adverse temperature gradient has been investigated extensively considering local thermal equilibrium (LTE) model. Recently, there has been a great upsurge of interest in understanding this convective instability problem using local thermal non-equilibrium (LTNE) model because of its relevance and applications in many practical situations such as convection in stellar atmospheres, nuclear reactor maintenance, heat exchangers, processing of composite materials, resin flow, fuel cells, tube refrigerators in space, flows in microchannels and porous metallic foams to mention a few [1, 2].

In the LTNE model two temperature equations, one for fluid medium and one for solid medium, are used and it appears that the continuum theories for LTNE effects have started in the late 1990s [3–5]. Taking into account LTNE effects, Banu and Rees [6] and Malashetty et al. [7] discussed thermal convection in a porous medium, while Straughan [8] demonstrated the equivalence of linear instability threshold with global nonlinear stability threshold for convection. Since then several investigations have been undertaken on the said problem accounting for additional effects such as rotation [8, 9], variable viscosity and density maximum [10], non-uniform temperature gradients [11, 12], solute concentration [13] and volumetric heat generation [14]. The growing volume of work devoted to this area is well documented in the books by Vafai [15] and Nield and Bejan [16].

The classical energy equation used in the study of convective instability problems in a fluid/porous layer is a parabolic-type partial differential equation which allows an infinite-speed for heat transport. The new theories make use of modified versions that involve hyperbolic-type heat transport equation admitting finite-speed for heat transport. Thus, heat transport is viewed as a wave phenomenon rather than a diffusion phenomenon and this is referred to as second sound. In particular, the second sound effect appears greater in solids, especially those involved in porous metallic foams. A key way to introduce this effect is to use Cattaneo [17] law for the heat flux. Based on this approach, studies have been undertaken in the past to investigate thermal convection in a fluid layer [18, 19] and also in a fluid-saturated Darcy porous medium using a local thermal equilibrium (LTE) model with Cattaneo–Fox and Cattaneo–Christov effects [20,

21]. The details about the developments on this topic are amply documented in the book by Straughan [22]. The Cattaneo effect on thermal convection in a fluid-saturated Darcy porous medium using a local thermal non-equilibrium (LTNE) model is investigated for the first time by Straughan [2]. In addition to performing linear instability analysis, a global nonlinear stability threshold is determined. The effect of second sound is delineated in a detailed manner. A review on thermal instability in a Brinkman porous medium incorporating fluid inertia and Cattaneo–Christov theory in the constitutive equation for heat flux is presented by Haddad [23] for LTE model.

It is known that high porosity porous materials (for example, foam metals) are used in industrial applications such as heat exchangers, chemical reactors and fluid filters. Hence, high porosity materials are of much current interest in industry. They are typically man-made and are important in the design of heat transfer devices. In dealing such highly porous materials the use of the higher order Darcy–Brinkman equation becomes more appropriate to model the fluid flow, as opposed to the more commonly used Darcy's law [24]. Some of the works to deal with this extension are by Georgiadis and Catton [25], Kladias and Prasad [26] and Kelliher et al. [27]. Shivakumara et al. [28] investigated the effects of boundary and local thermal non-equilibrium on the criterion for the onset of convection in a sparsely packed horizontal anisotropic porous layer. Many more works are available on the non-Darcy–Benard convection in a porous medium and the details can be found in the books by Straughan [29] and Nield and Bejan [16].

Nonetheless, no attention has been given to understand the influence of Cattaneo effect in the solid on thermal convective instability in high porosity porous materials despite its occurrence and importance in many practical problems as mentioned above. The intent of the present paper is to investigate this problem in a layer of Newtonian fluid-saturated Brinkman porous medium using a LTNE model, which allows the fluid and solid media to be at different temperatures, and including fluid inertia. As considered by Straughan [2], the usual Fourier heat-transfer law is retained in the fluid phase while temperature waves are allowed in the solid phase via a Cattaneo-like heat flux theory as the second sound effect is dominant in the solid skeleton. Although the linear stability analysis is modified, it is still possible to proceed analytically to find the condition for the onset of convection. This work is more general in the sense that the results for the Darcy case can be recovered when the Brinkman or effective viscosity is zero.

2. Mathematical Formulation

We consider a horizontal layer of Brinkman porous medium of thickness d. The lower surface is held at constant temperature T_l, while the upper surface is at T_u ($<T_l$). A Cartesian coordinate system (x, y, z) is chosen such that the origin is at the bottom of the porous layer and the z-axis vertically upward in the presence of gravitational field. The solid and fluid phases of the porous medium are assumed to be in local thermal non-equilibrium (LTNE) with a two-field model for temperatures. The solid temperature equation is modified to allow the heat transfer via a Cattaneo heat flux theory, while the usual Fourier heat-transfer law is used in the fluid. The basic equations governing the flow of an incompressible fluid saturating a layer of Brinkman porous medium with LTNE and Cattaneo effect in the solid are [2, 16]

$$\nabla.\vec{q} = 0 \tag{1}$$

$$\rho_0\left[\frac{1}{\varepsilon}\frac{\partial\vec{q}}{\partial t}+\frac{1}{\varepsilon^2}(\vec{q}.\nabla)\vec{q}\right]=-\nabla p+\rho_f\vec{g}-\frac{\mu_f}{K}\vec{q}+\tilde{\mu}_f\nabla^2\vec{q} \tag{2}$$

$$\varepsilon\left(\rho_0 c\right)_f\frac{\partial T_f}{\partial t}+\left(\rho_0 c\right)_f\left(\vec{q}\cdot\nabla\right)T_f=\varepsilon k_f\nabla^2T_f+h\left(T_s-T_f\right) \tag{3}$$

$$\left(1-\varepsilon\right)\left(\rho_0 c\right)_s\frac{\partial T_s}{\partial t}=-\left(1-\varepsilon\right)\nabla\cdot\vec{Q}-h\left(T_s-T_f\right) \tag{4}$$

$$\tau_s\frac{\partial\vec{Q}}{\partial t}=-\vec{Q}-k_s\nabla T_s \tag{5}$$

$$\rho_f=\rho_0\left\{1-\alpha_t\left(T_f-T_l\right)\right\}. \tag{6}$$

In the above equations, $\vec{q}=(u,v,w)$ the velocity vector, p the pressure, ρ_f the fluid density, μ_f the fluid viscosity, $\tilde{\mu}_f$ the effective viscosity, K the permeability of the porous medium, ε the porosity of the medium, $\vec{g}$ the gravitational acceleration, T_f the temperature of the fluid, T_s the temperature of the solid, $\vec{Q}$ the heat flux in the solid, c the specific heat at constant pressure, k_f the thermal conductivity of the fluid, k_s the thermal conductivity of the solid, h the inter-phase heat transfer coefficient which depends on the nature of the porous matrix and the saturating fluid, τ_s the solid thermal relaxation time, α_t the coefficient of thermal expansion and ρ_0 the reference density. A subscript s or f refers to the solid or fluid, respectively.

The basic state is quiescent and there exists the following solution for the basic state:

$$\vec{q}_b = 0\,,\; p_b(z) = p_0 - \rho_0 g\, z - \frac{1}{2}\rho_0 \alpha_t g \beta\, z^2\,,\; T_{fb} = T_{sb} = -\beta z + T_l\,,\; \vec{Q}_b = \left(0, 0, k_s \beta\right) \tag{7}$$

where $\beta = \Delta T / d = (T_l - T_u)/d$ is the temperature gradient and the subscript *b* denotes the basic state. It may be noted that the fluid and solid phases have the same temperatures at the bounding surfaces of the porous layer.

3. Linear Stability Theory

To investigate the conditions under which the convection arises against small disturbances, we consider a perturbed state in the form

$$\vec{q} = \vec{q}'\,,\; p = p_b(z) + p'\,,\; T_f = T_{fb}(z) + T_f'\,,\; T_s = T_{sb}(z) + T_s'\,,\; \vec{Q} = \vec{Q}_b(z) + \vec{Q}' \tag{8}$$

where $\vec{q}'=(u', v', w')$, p', T_f', T_s' and $\vec{Q}' = (Q'_x, Q'_y, Q'_z)$ are the perturbed variables and are assumed to be small. Substituting Eq. (8) into momentum Eq. (2), linearizing, eliminating the pressure term by taking curl twice, the *z*-component of the resulting equation can be obtained as follows (after dropping the primes):

$$\left(\frac{\rho_0}{\varepsilon}\frac{\partial}{\partial t} + \frac{\mu_f}{K} - \tilde{\mu}_f \nabla^2\right)\nabla^2 w = \rho_0 \alpha_t g \nabla_h^2 T_f \tag{9}$$

where $\nabla_h^2 = \partial^2/\partial x^2 + \partial^2/\partial y^2$ is the horizontal Laplacian operator. Equations (3) and (4), after using (8) and linearizing, take the following form (after dropping the primes):

$$\varepsilon\left(\rho_0 c\right)_f \frac{\partial T_f}{\partial t} + \left(\rho_0 c\right)_f w \frac{dT_{fb}}{dz} = \varepsilon k_f \nabla^2 T_f + h\left(T_s - T_f\right) \tag{10}$$

$$\left(1-\varepsilon\right)\left(\rho_0 c\right)_s \frac{\partial T_s}{\partial t} = -\left(1-\varepsilon\right)\nabla\cdot\vec{Q} - h\left(T_s - T_f\right). \tag{11}$$

Equation (5), after substituting (8), becomes (after dropping the primes)

$$\tau_s \frac{\partial \vec{Q}}{\partial t} = -\vec{Q} - k_s \nabla T_s\,. \tag{12}$$

It is convenient to eliminate $\vec{Q}$ from Eq. (11), upon using Eq. (12), to get

$$\left(1-\varepsilon\right)\left(\rho_0 c\right)_s \left(\tau_s \frac{\partial}{\partial t} + 1\right)\frac{\partial T_s}{\partial t} = \left(1-\varepsilon\right)k_s \nabla^2 T_s - h\left(\tau_s \frac{\partial}{\partial t} + 1\right)\left(T_s - T_f\right). \tag{13}$$

It is seen that Eq. (13) is effectively hyperbolic and oscillatory instability may be possible with increasing τ_s. Equation (13) becomes parabolic when $\tau_s = 0$.

The normal mode expansion of the dependent variables is assumed in the form

$$\left\{w, T_f, T_s\right\} = \left\{W(z), \Theta(z), \Phi(z)\right\} \exp\left[i(\ell x + my) + \sigma t\right] \tag{14}$$

where ℓ and m are wave numbers in the x and y directions, respectively, $W(z)$ is the amplitude of vertical component of perturbed velocity, $\Theta(z)$ is the amplitude of perturbed fluid temperature, $\Phi(z)$ is the amplitude of perturbed solid temperature and σ is the growth rate. Substituting Eq. (14) into Eqs. (9), (10) and (13), and non-dimensionalizing the variables by setting

$$\left(x^*, y^*, z^*\right) = \left(\frac{x^*}{d}, \frac{y^*}{d}, \frac{z^*}{d}\right),\ t^* = \frac{\kappa_f}{d^2} t,\ \ W^* = \frac{d}{\varepsilon \kappa_f} W,\ \ \Theta^* = \frac{1}{\beta d}\ \Theta,\ \ \Phi^* = \frac{1}{\beta d}\ \Phi \tag{15}$$

where $\kappa_f = k_f / \left(\rho_0 c\right)_f$ is the effective thermal diffusivity of the fluid, we obtain the following dimensionless equations (after dropping the primes):

$$\left[\frac{\sigma}{Pr_D} + 1 - Da\left(D^2 - a^2\right)\right]\left(D^2 - a^2\right) W = -a^2 R_D \Theta \tag{16}$$

$$\sigma \Theta - \left(D^2 - a^2\right)\Theta - H\left(\Phi - \Theta\right) = W \tag{17}$$

$$\left[\alpha\sigma\left(\tau\sigma + 1\right) - \left(D^2 - a^2\right)\right]\Phi + \gamma H\left(\tau\sigma + 1\right)\left(\Phi - \Theta\right) = 0\,. \tag{18}$$

Here, $D = d / dz$ is the differential operator, $a = \sqrt{\ell^2 + m^2}$ is the overall horizontal wave number, $R_D = \rho_0 \alpha_t g \beta K d^2 / \varepsilon \mu_f \kappa_f$ is the Darcy-Rayleigh number and it is a ratio of buoyant to viscous forces, $Da = \tilde{\mu}_f K / \mu_f d^2$ is the Darcy number, $Pr_D = Pr\varepsilon / Da$ is the Darcy-Prandtl number or the Vadasz number, $H = hd^2 / \varepsilon k_f$ is the scaled inter-phase heat transfer coefficient, $\gamma = \varepsilon k_f / \left(1 - \varepsilon\right) k_s$ is the porosity modified conductivity ratio, $\tau = \tau_s \kappa_f / d^2$ is the non-dimensional solid thermal relaxation time parameter and $\alpha = \left(\rho_0 c\right)_s k_f / \left(\rho_0 c\right)_f\ k_s$ is the ratio of conductivities.

Equations (16)–(18) are to be solved subject to appropriate boundary conditions. Analytical progress is facilitated by taking stress-free isothermal boundaries.

The boundary conditions are:

$$W = D^2W = \Theta = \Phi = 0 \quad \text{at} \quad z = 0, 1. \tag{19}$$

Equations (16)-(18) admit solution satisfying the boundary conditions in the form

$$W = A_1 \sin \pi z\,,\ \Theta = A_2 \sin \pi z\,,\ \Phi = A_3 \sin \pi z \tag{20}$$

where A_1 - A_3 are constants. Substituting Eq. (20) into Eqs. (16)–(18) and eliminating the constants A_1 - A_3 from the resulting equations yields the following characteristic equation:

$$\begin{vmatrix} \left(\dfrac{\sigma}{Pr_D} + 1 + Da\delta\right)\delta & -a^2 R_D & 0 \\ 1 & -(\sigma + \delta + H) & H \\ 0 & -\gamma H(\tau\sigma + 1) & \delta + (\tau\sigma + 1)(\sigma\alpha + \gamma H) \end{vmatrix} = 0 \tag{21}$$

where $\delta = \pi^2 + a^2$. One of the ways in which Eq. (21) may be used to examine the stability of the system will now be discussed. All the parameters, except the Darcy-Rayleigh number R_D, are taken as given. Expanding the determinant gives the following expression for R_D:

$$R_D = \frac{\delta\left(Pr_D + Da\,Pr_D\delta + \sigma\right)\left[(\sigma + \delta + H)\left\{\delta + (\alpha\sigma + H\gamma)(\tau\sigma + 1)\right\} - H^2\gamma(\tau\sigma + 1)\right]}{Pr_D\, a^2\left\{\delta + (\tau\sigma + 1)(H\gamma + \alpha\sigma)\right\}}. \tag{22}$$

To examine the stability of the system, the real part of σ is set to zero and we take $\sigma = i\omega$. Substituting $\sigma = i\omega$ in Eq. (22) and clearing the complex quantities from the denominator, we get

$$R_D = \frac{\delta}{Pr_D\, a^2\left\{2H\gamma\delta + \delta^2 - 2\tau\alpha\delta\omega^2 + \left(H^2\gamma^2 + \alpha^2\omega^2\right)\left(1 + \tau^2\omega^2\right)\right\}}\left(\Delta_1 + i\omega\Delta_2\right) \tag{23}$$

where

$$\Delta_1 = \left\{Pr_D\delta\left(1+Da\delta\right)-\omega^2\right\}\left\{\delta^2-2\tau\alpha\delta\omega^2+\alpha^2\omega^2\left(1+\tau^2\omega^2\right)\right\}$$
$$+H^2\gamma\left\{Pr_D\delta\left(1+Da\delta\right)\left(1+\gamma+\tau^2\gamma\omega^2\right)-\omega^2\left(\alpha+\gamma-\tau\delta+\tau^2\omega^2\left(\alpha+\gamma\right)\right)\right\}$$
$$+H\left\{Pr_D\delta\left(1+Da\delta\right)\left(\delta^2\left(1+2\gamma\right)-2\tau\alpha\delta\omega^2+\alpha^2\omega^2\left(1+\tau^2\omega^2\right)\right)-2\gamma\delta\omega^2\right\}$$

$$\Delta_2 = \left\{Pr_D+\delta+Pr_DDa\delta\right\}\left\{\delta^2-2\tau\alpha\delta\omega^2+\alpha^2\omega^2\left(1+\tau^2\omega^2\right)\right\}$$
$$+H^2\gamma\left\{\delta\left(1+\gamma+\tau^2\gamma\omega^2\right)+Pr_D\left(1+Da\delta\right)\left(\alpha+\gamma-\tau\delta+\tau^2\omega^2\left(\alpha+\gamma\right)\right)\right\}$$
$$+H\left\{\delta^2\left(1+2\gamma\right)+2Pr_D\gamma\delta\left(1+Da\delta\right)-2\tau\alpha\delta\omega^2+\alpha^2\omega^2\left(1+\tau^2\omega^2\right)\right\}.$$

Since the Rayleigh number R_D is a physical quantity, it must be real. Hence, from Eq. (23) it implies either $\omega = 0$ or $\Delta_2 = 0$ $\left(\omega \neq 0\right)$, and accordingly the condition for the onset of stationary and oscillatory convection is obtained.

3.1. Stationary convection $\left(\omega = 0\right)$

The stationary convection (direct bifurcation) corresponds to $\omega = 0$. Substituting $\omega = 0$ in Eq. (23), we note that the stationary convection occurs at $R_D = R_D^s$, where

$$R_D^s = \frac{\delta^2\left(1+\delta Da\right)\left\{H\left(1+\gamma\right)+\delta\right\}}{a^2\left(\delta+\gamma H\right)}. \tag{24}$$

From the above expression it is obvious that the onset of stationary convection is independent of Cattaneo effect and Eq. (24) coincides with the expression obtained by Malashetty et al. [7]. The stationary Rayleigh number R_D^s given by Eq. (24) attains the critical value R_{Dc}^s at $a^2 = a_c^2$, where a_c^2 satisfies the equation

$$b_1\left(a_c^2\right)^5+b_2\left(a_c^2\right)^4+b_3\left(a_c^2\right)^3+b_4\left(a_c^2\right)^2+b_5\left(a_c^2\right)+b_6 = 0 \tag{25}$$

where

$$b_1 = 2Da$$
$$b_2 = \left\{1+Da\left(H+7\pi^2+4H\gamma\right)\right\}$$
$$b_3 = 2\left(\pi^2+H\gamma\right)\left\{1+Da\left(H+4\pi^2+H\gamma\right)\right\}$$

$$b_4 = \left\{2Da\pi^6 + H^2\left(1+3Da\pi^2\right)\gamma\left(1+\gamma\right) - H\pi^2\left(1-2\left(1+3Da\pi^2\right)\gamma\right)\right\}$$

$$b_5 = -2\pi^4\left(1+Da\pi^2\right)\left(H+\pi^2+H\gamma\right)$$

$$b_6 = -\pi^4\left(1+Da\pi^2\right)\left\{\pi^4 + H^2\gamma\left(1+\gamma\right) + H\pi^2\left(1+2\gamma\right)\right\}.$$

Equation (25) is solved numerically for various values of γ, Da and H, and the critical value of a_c^2 is obtained. Using this a_c^2 in Eq. (24), the critical Rayleigh number R_{Dc}^s is obtained, above which the stationary convection sets in. It is interesting to check Eq. (24) under some limiting cases. When $Da = 0$ (i.e. $\tilde{\mu} = 0$), Eq. (24) reduces to

$$R_D^s = \frac{\delta^2 H\left(1+\gamma\right)+\delta^3}{a^2\left(\delta+\gamma H\right)}. \tag{26}$$

The above expression is the same as the one obtained by Banu and Rees [6] and Straughan [2]. When $Da = 0 = H$, Eq. (24) simply reduces to

$$R_D^s = \frac{\delta^2}{a^2}. \tag{27}$$

Evidently, R_D^s given by Eq. (27) attains its minimum at $a = \pi$. That is, the critical Darcy-Rayleigh number is $4\pi^2$ and the associated critical wave number is π ; the known results for the classical Darcy-Benard problem.

3.2. Oscillatory convection $\left(\omega \neq 0, \Delta_2 = 0\right)$

The oscillatory onset corresponds to $\Delta_2 = 0\,(\omega \neq 0)$ in Eq. (23) and this condition gives a dispersion relation of the form

$$B_1\left(\omega^2\right)^2 + B_2\left(\omega^2\right) + B_3 = 0 \tag{28}$$

where

$$B_1 = \tau^2\alpha^2\left(H + Pr_D + \delta + Da\,Pr_D\delta\right)$$

$$B_2 = \left(\alpha - 2\tau\delta\right)\left\{H\alpha + \alpha\left(Pr_D + \delta + DaPr_D\delta\right)\right\} + H^2\tau^2\gamma\left\{\gamma\delta + Pr_D\left(\alpha+\gamma\right)\left(1+Da\delta\right)\right\}$$

$$B_3 = \delta^2\left(Pr_D + \delta + DaPr_D\delta\right) + H^2\gamma\left\{\left(1+\gamma\right)\delta + Pr_D\left(1+Da\delta\right)\left(\gamma+\alpha-\tau\delta\right)\right\}$$
$$+ H\delta\left\{\delta + 2\gamma\delta + 2Pr_D\gamma\left(1+Da\delta\right)\right\}.$$

For the occurrence of oscillatory convection, ω^2 should be positive. From Eq. (28), it is observed that the coefficient B_1 is always positive while the coefficients B_2 and/or B_3 can be negative depending on the choices of parametric values. If this is the case, then from Descartes' rule of signs it follows that one or two positive values of ω^2 exist indicating the occurrence of oscillatory convection for those choices of parametric values. However, if τ =0 (i.e. in the absence of Cattaneo effect in the solid) then it is noted that both B_2 and B_3 are positive and the occurrence of oscillatory convection is ruled out. Thus, it is evident that the Cattaneo effect in the solid is to initiate the occurrence of convective instability via oscillatory convection as well in lieu of stationary convection.

The oscillatory convection occurs at $R_D = R_D^o$, where

$$R_D^o = \frac{\delta\Delta_1}{Pr_D\, a^2 \left\{2H\gamma\delta + \delta^2 - 2\tau\alpha\delta\omega^2 + \left(H^2\gamma^2 + \alpha^2\omega^2\right)\left(1+\tau^2\omega^2\right)\right\}} \tag{29}$$

and ω^2 is given by Eq. (28). The critical oscillatory Darcy-Rayleigh number R_{Dc}^o with respect to the wave number is computed numerically as follows. Equation (28) is solved first to determine the positive values of ω^2 for chosen parametric values. If there are none, then no oscillatory convection is possible. If there is only one positive value of ω^2 then the critical value of R_D^o with respect to the wave number is computed numerically from Eq. (29). If there are two positive values of ω^2, then the least of R_D^o amongst these two ω^2 is retained to find the critical value of R_D^o with respect to the wave number.

5. Results and discussion

The onset of thermal convective instability in a layer of fluid-saturated Brinkman porous medium is investigated using a local thermal non-equilibrium (LTNE) model with Cattaneo effect in the solid. It is observed that the presence of Cattaneo effect is to instigate the occurrence of convective instability via oscillatory motions under certain conditions and in the absence of such effects it is established [7] that the instability occurs always via stationary convection. The condition for the occurrence of stationary and oscillatory onset is established analytically and the results are discussed graphically for different values of physical parameters namely, the solid thermal

relaxation time parameter τ, the Darcy number Da, the Darcy-Prandtl number or the Vadasz number Pr_D, the inter-phase heat transfer coefficient H, the ratio of conductivities α and the porosity modified conductivity ratio γ. In addition, the results are also presented for copper oxide and aluminium oxide solid skeletons as both materials have practical use in heat exchangers.

The neutral stability curves on the (R_D, a^2)–plane are demonstrated for different values of τ (with $\alpha = 1, Pr_D = 20$), Pr_D (with $\alpha = 1, \tau = 0.5$) and α (with $Pr_D = 20, \tau = 0.5$) in Figs. 1(a), (b) and (c), respectively at $\gamma = 1$, $Da = 1$ and $H = 10$. The neutral curves exhibit a single minimum with respect to the wave number and they are similar to those observed in the standard Brinkman LTNE model. From the figures it is seen that the parameters τ, Pr_D and α affect only the onset of oscillatory convection. Moreover, increase in τ and Pr_D is to decrease the region of stability, while an opposite trend is noticed with increasing α. A closer inspection of the figures further reveals that there exists a threshold value of τ $(=\tau^*)$, Pr_D $(= Pr_D^*)$ and α $(=\alpha^*)$ below which only oscillatory convection is preferred. For the chosen parametric values, it is found that $\tau^* = 0.5114$ (Fig. 1a), $Pr_D^* = 34.24$ (Fig. 1b) and $\alpha^* = 0.824$ (Fig. 1c).

The critical Darcy-Rayleigh number for the onset of stationary (R_{Dc}^s) and oscillatory (R_{Dc}^O) convection, the corresponding critical wave number (a_c^2) and the critical frequency of oscillation (ω_c^2) are computed numerically for various values of physical parameters and the results are summarized in Figs. 2–7. Figures 2(a), (b) and (c) show the variation of critical Darcy-Rayleigh numbers, the critical wave number and the critical frequency of oscillation, respectively as a function of H for different values of τ (= 0.5, 1 and 10) and for two values of Pr_D (= 20 and 200) and Da (= 0.5 and 1). In Figs. 3(a-c), the results are exhibited for the same set of parametric values as considered in Figs. 2 (a-c) but for changed values of Da = 10 and 15.

Figure 2(a) shows that, depending on the parametric values, convective instability occurs via oscillatory convection when H exceeds a threshold value H^T, and this value increases significantly with decreasing τ. Besides, the effect of inter-phase heat-transfer coefficient H on the nature of convective instability is not coherent. It is noted that the onset of stationary convection is delayed, while the onset of oscillatory convection is hastened with increasing H.

Moreover, the influence of H on the oscillatory onset is more noticeable in the beginning and thereafter its effect becomes fairly insensitive. It is seen that this behavior is more so when τ = 10. Although an increase in the Prandtl number is to hasten the onset of oscillatory convection, its influence goes on diminishing as the value of τ increases. It is noted that the influence of Pr_D on the onset of oscillatory convection is completely subdued when τ assumes the value 10. The onset of both stationary and oscillatory convection is delayed as the value of Da increases (equivalently increase in the ratio of viscosities, $\tilde{\mu}_f / \mu_f$) due to an increase in the viscous diffusion. Further, it is seen that the value of H^T decreases marginally with increasing Pr_D and Da.

The variation of critical wave number as a function of H is exhibited in Fig. 2(b). It is seen that the critical wave number for the oscillatory convection (denoted by o) starts beyond threshold values of H. The values of a_c^2 increase sharply with H initially and become almost insensitive with further increase in H and this trend is more predominant at τ =10. Thus the size of convection cells decreases with increasing H, while increasing τ, Da and Pr_D is to decrease a_c^2 and hence their effect is to enlarge the size of convection cells. It is also observed that the values of a_c^2 for stationary convection are higher than those of oscillatory convection for τ =1 and 10.

The critical frequency of oscillations ω_c^2 displayed in Fig. 2(c) shows that the variation in ω_c^2 with H is significant for τ = 0.5 and 1, while this trend is found to be not so significant for τ = 10. The effect of increasing Da and Pr_D is to increase ω_c^2 when τ = 0.5 and 1, but for τ = 10 these two parameters do not show any influence on ω_c^2. The results presented for relatively higher values of Da =10 and 15 in Figs. 3(a-c) exhibit similar kind of behavior as noticed in Figs. 2(a-c). But, we find that the effect of Prandtl number on R_{Dc}^O (Fig. 3a), a_c^2 (Fig. 3b) and ω_c^2 (Fig. 3c) is found to be insignificant for all values of τ considered.

The impact of conductivity ratio α on the stability characteristics of the system is displayed in Figs. 4(a-c) for Da = 0.5 and 1and in Figs. 5(a-c) for Da = 10 and 15 as a function of

H for selected values of τ at Pr_D =20 and $\gamma = 1$. From the figures, it is seen that the effect of increasing α is to delay the onset of oscillatory convection and thereby to increase the value of H^T (Fig. 4a). Also, the effect of α on the onset of oscillatory convection diminishes with increasing τ. The critical wave number increases with α indicating its effect is to decrease the size of convection cells (Fig. 4b). For a fixed value of τ, ω_c^2 decreases with increasing α and also decrease in Da (Fig. 4c). The results shown in Fig. 5(a) for Da = 10 and 15 corroborate the results observed in Fig. 4(a). However, it is seen that there is no impact of α on a_c^2 (Fig. 5b) and ω_c^2 (Fig. 5c) with varying H for values of τ considered.

The values of α and γ for copper oxide (CuO) and aluminium oxide (Al_2O_3) solid skeletons are given by Straughan [20]:

$$\alpha_{CuO} = 8.664\times10^{-4}, \gamma_{CuO} = 6.403\times10^{-4} \text{ and } \alpha_{Al_2O_3} = 1.420\times10^{-2},\ \gamma_{Al_2O_3} = 7.337\times10^{-3}.$$

For these two sets of parametric values, the results are displayed in Figs. 6 and 7 for two values of τ (= 9, 10) and Da (= 5, 10) at $Pr_D = 20$. It is observed that oscillatory convection is preferred at relatively high values of H when compared to values of α =1 and γ =1 considered in Figs. 2 and 3. This demonstrates the interplay of various physical parameters in the occurrence of oscillatory convection due to the presence of Cattaneo effect in the solid. As expected, increase in the value of Da is to delay the onset of convection, but its effect on a_c^2 and ω_c^2 is found to be not so significant (Figs. 6a and 7a). The critical wave number increases with increasing H. That is, the size of the convection cells decreases in the (x, y)-plane. The critical wave number for the oscillatory convection is lower than that of stationary convection for values of τ considered indicating the cell size changes by a large amount to a much wider cell (Figs. 6b and 7b). The variation of ω_c^2 with H is illustrated in Figs. 6(c) and 7(c). From the figures it is observed that increasing H is to increase ω_c^2. Also, increase in Da is to increase ω_c^2 for a fixed value of τ. Nonetheless, the parameter τ exhibits a dual effect on ω_c^2 with increasing H. Initially, increase in τ from 9 to 10 is to increase ω_c^2 up to a certain value of H for a fixed value of Da, and thereafter an opposite behavior could be seen.

The values of H^T at which the transition from stationary to oscillatory convection takes place and the corresponding critical oscillatory Rayleigh number, critical wave number, critical frequency of oscillations are tabulated in Table 1 for different values of Pr_D, α and γ at $Da = 1$ and $\tau = 1$. In Table 2, similar results are presented for different values of τ at $Da = 10$ and $Pr_D = 20$. In these tables the results are provided for copper oxide and aluminium oxide solid skeletons as well. From Table 1, it is noted that increasing Pr_D is to decrease R_{Dc}^O, H^T and the least for $Pr_D \to \infty$; the results which correspond to the absence of fluid inertia. Furthermore, increase in the value of τ is to reduce R_{Dc}^O and the value of H^T (Table 2). The tabulated values in Table 1 and 2 also reveal that increase in the values of both α and γ is to reduce the values of R_{Dc}^O and H^T drastically.

6. Conclusions

The combined effect of a second sound and a local thermal non-equilibrium (LTNE) on the onset of thermal convection in a layer of fluid-saturated Brinkman porous medium is investigated considering fluid inertia. The second sound effect is considered in the solid via a Cattaneo heat flux theory and the usual Fourier heat-transfer law is used in the fluid. As a consequence the heat transfer in the solid is given by a hyperbolic-type of partial differential equation. The Cattaneo effect in the solid is found to alter the nature of convective instability and the condition for the occurrence of stationary and oscillatory convection is derived analytically. In contrast to the standard LTNE Brinkman model, the instability occurs via oscillatory convection when the solid thermal relaxation time parameter τ exceeds sufficiently high value. The effect of H is to delay the onset of stationary convection, while it exhibits an opposite trend on the onset of oscillatory convection. The threshold value of H, at which the transition from stationary to oscillatory convection takes place, decreases with increasing τ noticeably and marginally with increasing Pr_D and Da, while it increases with increasing α. The effect of increasing Da is to delay the onset of stationary and oscillatory convection, while increasing τ, Pr_D and decreasing α is to hasten the onset of oscillatory convection. The size of convection cells is enlarged with increasing τ, Da and Pr_D, but it is narrowed with increasing α.

References

[1] L.Virto, M. Carbonell, R. Castilla, P.J. Gamez-Montero, Heating of saturated porous media in practice: several causes of local thermal non-equilibrium, Int. J. Heat Mass Transfer 52 (2009) 5412–5422.

[2] B. Straughan, Porous convection with local thermal non-equilibrium temperatures and with Cattaneo effects in the solid, Proc. Royal Soc. A 469 (2013) 20130187.

[3] D.A. Nield, Effects of local thermal non-equilibrium in steady convection processes in saturated porous media: forced convection in a channel, J. Porous Med. 1 (1998) 181–186.

[4] W.J. Minkowycz, A. Haji-Sheikh, K. Vafai, On the departure from local thermal nonequilibrium in porous media due to a rapidly changing heat source: the Sparrow number. Int. J. Heat Mass Transfer 42 (1999) 3373–3385.

[5] F. Petit, F. Fichot, M. Quintard, Écoulement diphasique en milieu poreux: modèle à nonéquilibre local, Int. J. Thermal Sci. 38 (1999) 239–249.

[6] N. Banu, D.A.S. Rees, Onset of Darcy–Bénard convection using a thermal non-equilibrium model, Int. J. Heat Mass Transfer 45 (2002) 2221–2228.

[7] M.S. Malashetty, I.S. Shivakumara, S. Kulkarni, The onset of Lapwood–Brinkman convection using a thermal non-equilibrium model, Int. J. Heat Mass Transfer 48 (2005) 1155–1163.

[8] B. Straughan, Global nonlinear stability in porous convection with a thermal non-equilibrium model, Proc. Royal Soc. A 462 (2006) 409–418.

[9] M.S. Malashetty, M. Swamy, Effect of rotation on the onset of thermal convection in a sparsely packed porous layer using a thermal non-equilibrium model, Int. J. Heat Mass Transfer 53 (2010) 3088–3101.

[10] I.S. Shivakumara, A.L. Mamatha, M. Ravisha, Effects of variable viscosity and density maximum on the onset of Darcy-Benard convection using a thermal non-equilibrium model, J. Porous Med. 13 (2010) 613–622.

[11] J. Lee, I.S. Shivakumara, A.L. Mamatha, Effect of nonuniform temperature gradients on thermogravitational convection in a porous layer using a thermal nonequilibrium model, J. Porous Med. 14 (2011) 659–669.

[12] I.S. Shivakumara, J. Lee, K. Vajravelu, A.L. Mamatha, Effects of thermal nonequilibrium and non-uniform temperature gradients on the onset of convection in a heterogeneous porous medium, Int. Comm. Heat Mass Transfer 38 (2011) 906–910.

[13] M.S. Malashetty, M. Swamy, R. Heera, Double diffusive convection in a porous layer using a thermal non-equilibrium model, Int. J. Thermal Sci. 47 (2008) 1131–1147.

[14] A. Nouri-Borujerdi, A.R. Noghrehabadi, D.A.S. Rees, Onset of convection in a horizontal porous channel with uniform heat generation using a thermal non-equilibrium model, Transp. Porous Med. 69 (2007) 343–357.

[15] K. Vafai, Handbook of porous media. London: Taylor & Francis/CRC Press (2005).

[16] D.A. Nield, A. Bejan, Convection in porous media (4th Ed). New York: Springer (2013).

[17] C. Cattaneo, Sulla conduzione del calore, Atti Sem. Mat. Fis. Univ. Modena 3 (1948) 83–101.

[18] B. Straughan, F. Franchi, Bénard convection and the Cattaneo law of heat conduction, Proc. Royal Soc. Edinburgh A 96 (1984) 175–178.

[19] G. Lebon, A. Cloot, Bénard–Marangoni, instability in a Maxwell–Cattaneo fluid, Phys. Lett. A 105 (1984) 361–364.

[20] B. Straughan, Thermal convection with the Cattaneo–Christov model, Int. J. Heat Mass Transfer 53 (2010) 95–98.

[21] B. Straughan, Porous convection with Cattaneo heat flux, Int. J. Heat Mass Transfer 53 (2010) 2808–2812.

[22] B. Straughan, Heat waves, Series in Applied Math Science, 177, New York: Springer (2011).

[23] S.A.M. Haddad, Thermal instability in Brinkman porous media with Cattaneo-Christov heat flux, Int. J. Heat Mass Transfer 68 (2014) 659–668.

[24] A.A. Hill, B. Straughan, Global stability for thermal convection in a fluid overlying a highly porous material, Proc. Royal Soc. A 465 (2009) 207–217.

[25] J.G. Georgiadis, I. Catton, Prandtl number effect on Benard convection in a porous media, ASME J. Heat Transfer 108 (1986) 284–290.

[26] N. Kladias, V. Prasad, Experimental verification of Darcy–Brinkman–Forchheimer flow model for natural convection in porous media, J Theomorphic 5 (1991) 562–576.

[27] J.P. Kelliher, R. Temam, X. Wang, Boundary layer associated with the Darcy– Brinkman–Boussinesq model for convection in porous media, Physica D 240 (2011) 619–628.

[28] I.S. Shivakumara, J. Lee, A.L. Mamatha, M. Ravisha, Boundary and thermal non-equilibrium effects on convective instability in an anisotropic porous layer, J. Mech. Sci. Tech. 25 (2011) 911–921.

[29] B. Straughan, Stability and wave motion in porous media, Series in Applied Math Science, 165. New York: Springer (2008).

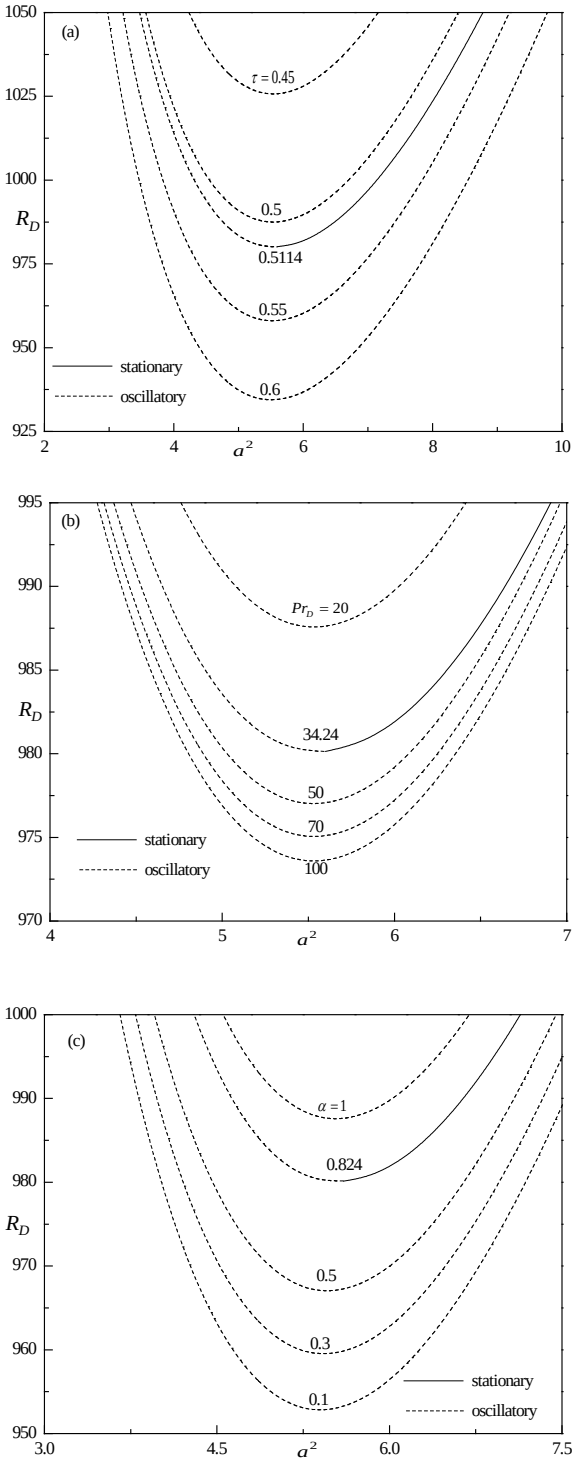

Fig. 1. Neutral curves for different values of **(a)** τ with $\alpha = 1$, $Pr_D = 20$, **(b)** Pr_D with $\alpha = 1$, $\tau = 0.5$, **(c)** α with $Pr_D = 20$, $\tau = 0.5$ when $\gamma = 1$, $Da = 1$ and $H = 10$.

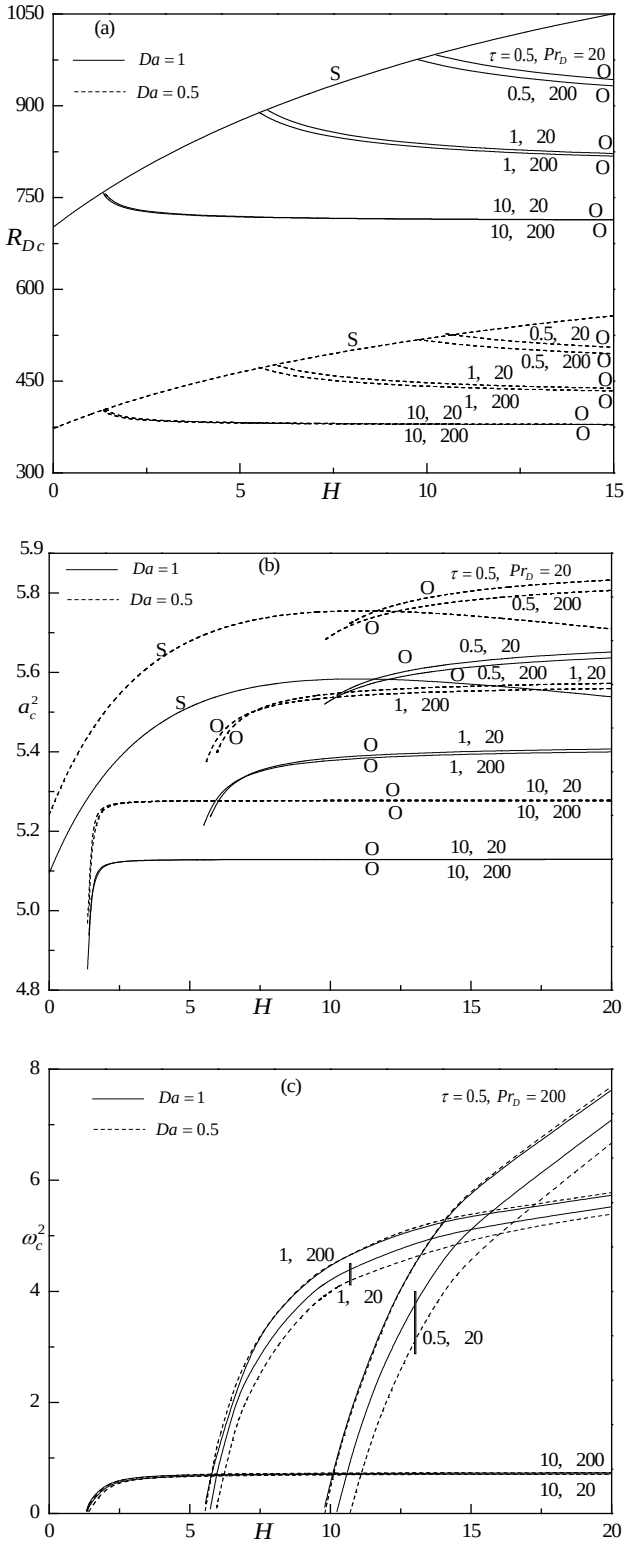

Fig. 2. Variation of **(a)** R_{Dc}, **(b)** a_c^2 : stationary (s), oscillatory(o), **(c)** ω_c^2 with H for two values of Da, Pr_D and three values of τ with $\gamma = 1$ and $\alpha = 1$.

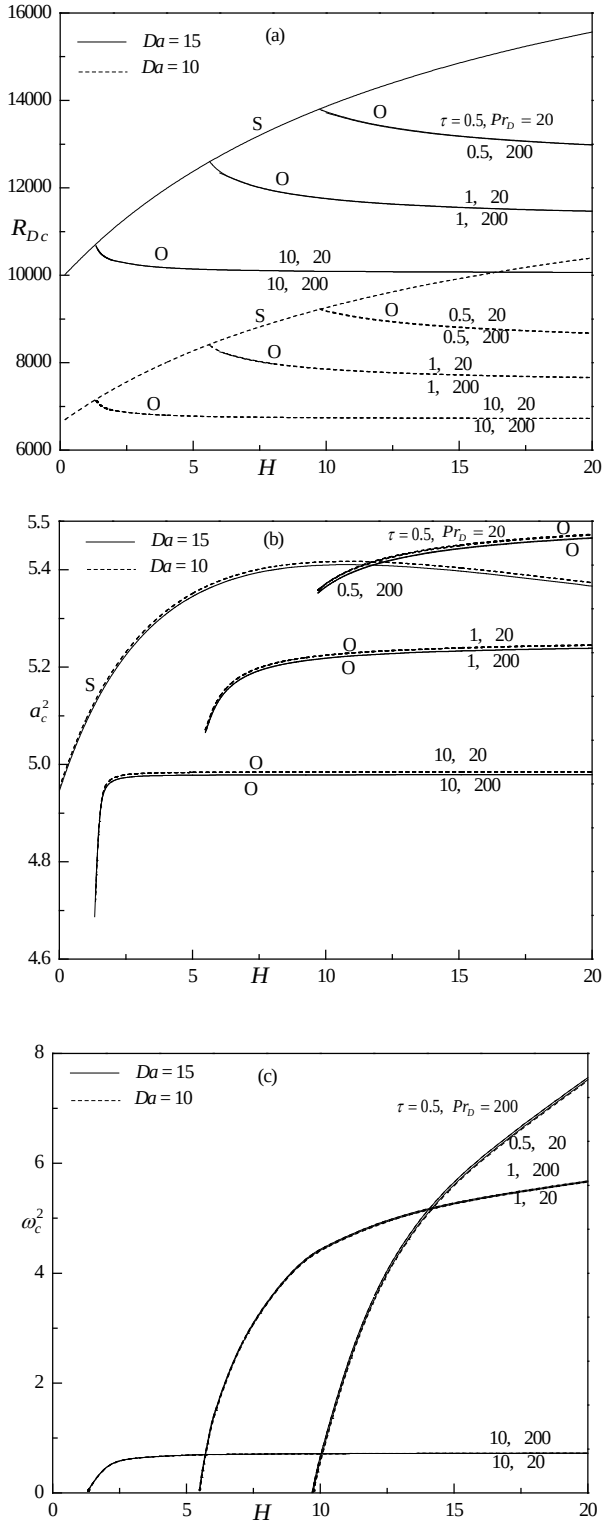

Fig. 3. Variation of **(a)** R_{Dc}, **(b)** a_c^2 : stationary (s), oscillatory(o), **(c)** ω_c^2 with H for two values of Da, Pr_D and three values of τ with $\gamma = 1$ and $\alpha = 1$.

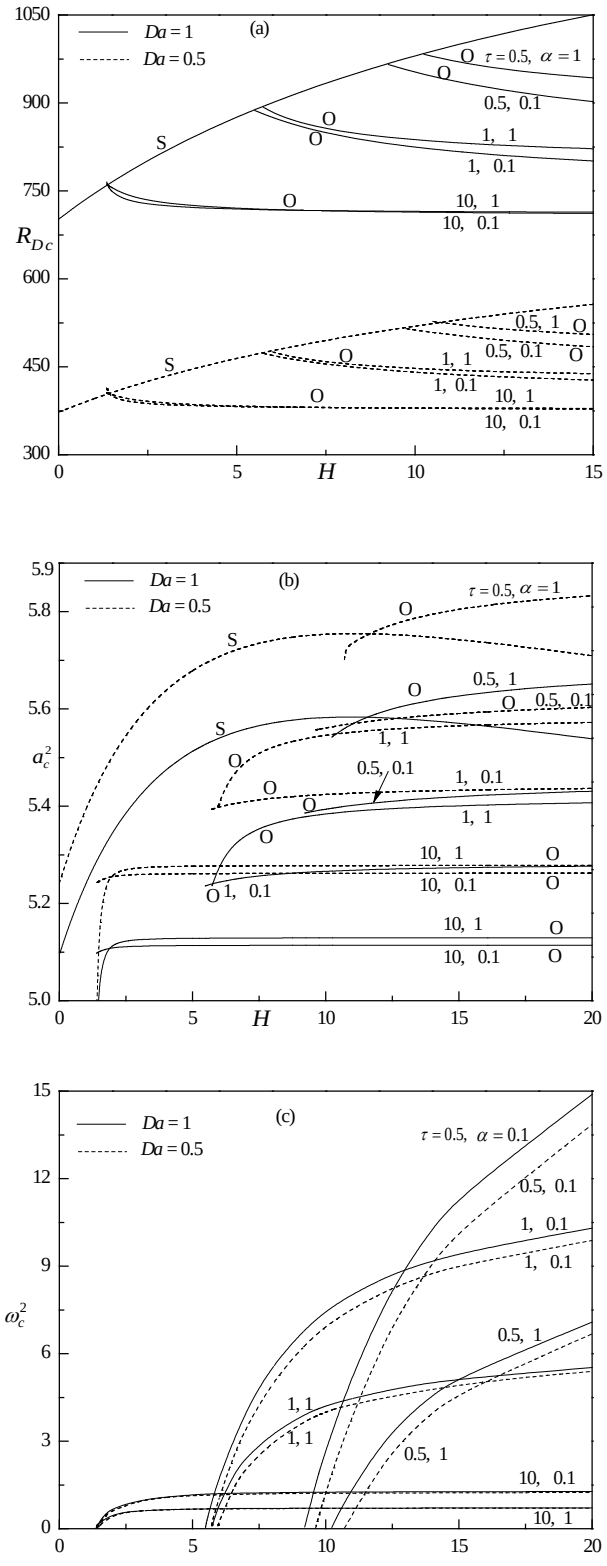

Fig. 4. Variation of **(a)** R_{Dc}, **(b)** a_c^2 : stationary (s), oscillatory(o), **(c)** ω_c^2 with H for two values of Da, α and three values of τ with $\gamma = 1$ and $Pr_D = 20$.

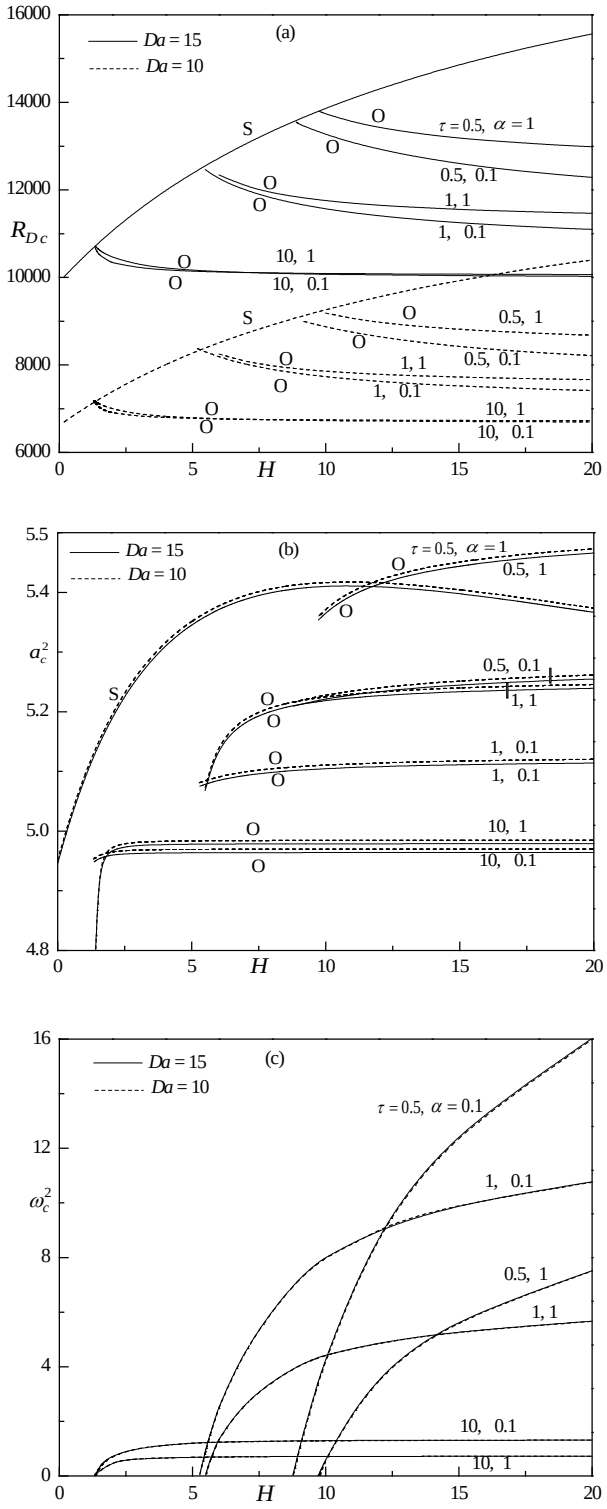

Fig. 5. Variation of **(a)** R_{Dc}, **(b)** a_c^2 : stationary (s), oscillatory(o), **(c)** ω_c^2 with H for two values of Da, α and three values of τ with $\gamma = 1$ and $Pr_D = 20$.

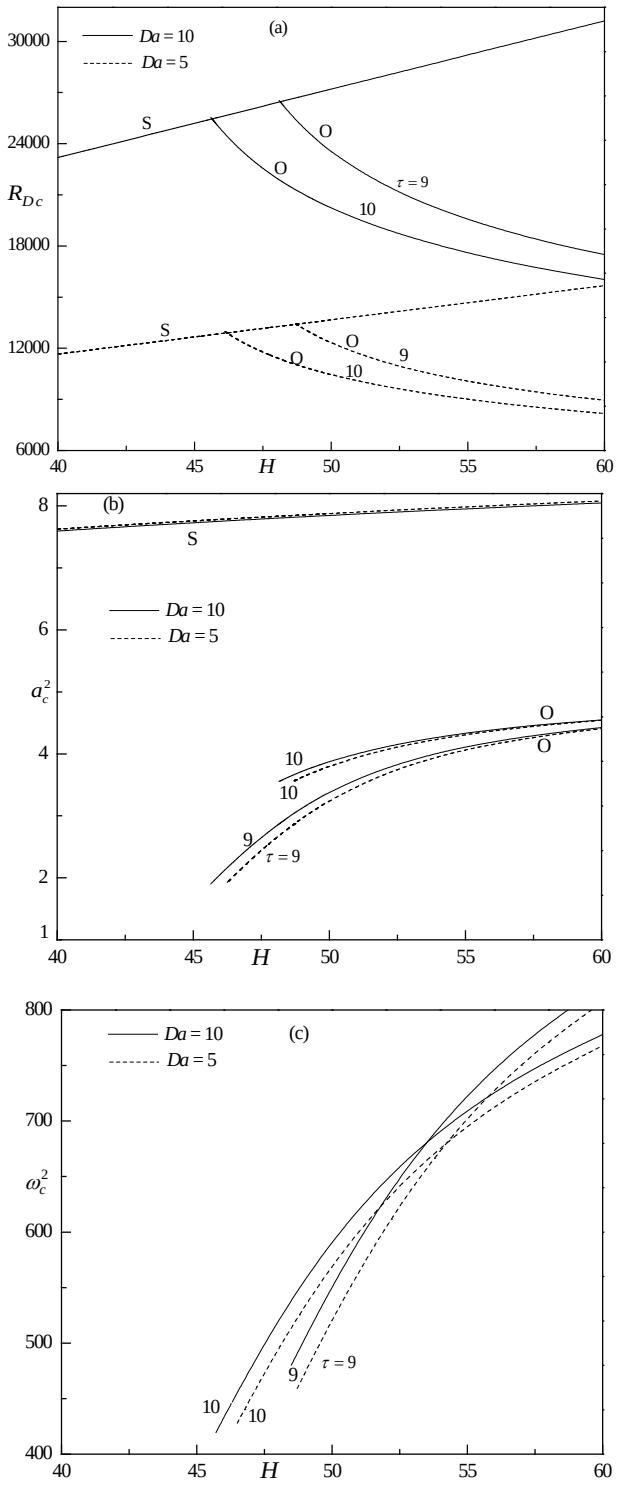

Fig. 6. Variation of **(a)** R_{Dc}, **(b)** a_c^2 : stationary (s), oscillatory(o), **(c)** ω_c^2 with H for *CuO* solid skeleton when $Pr_D = 20$.

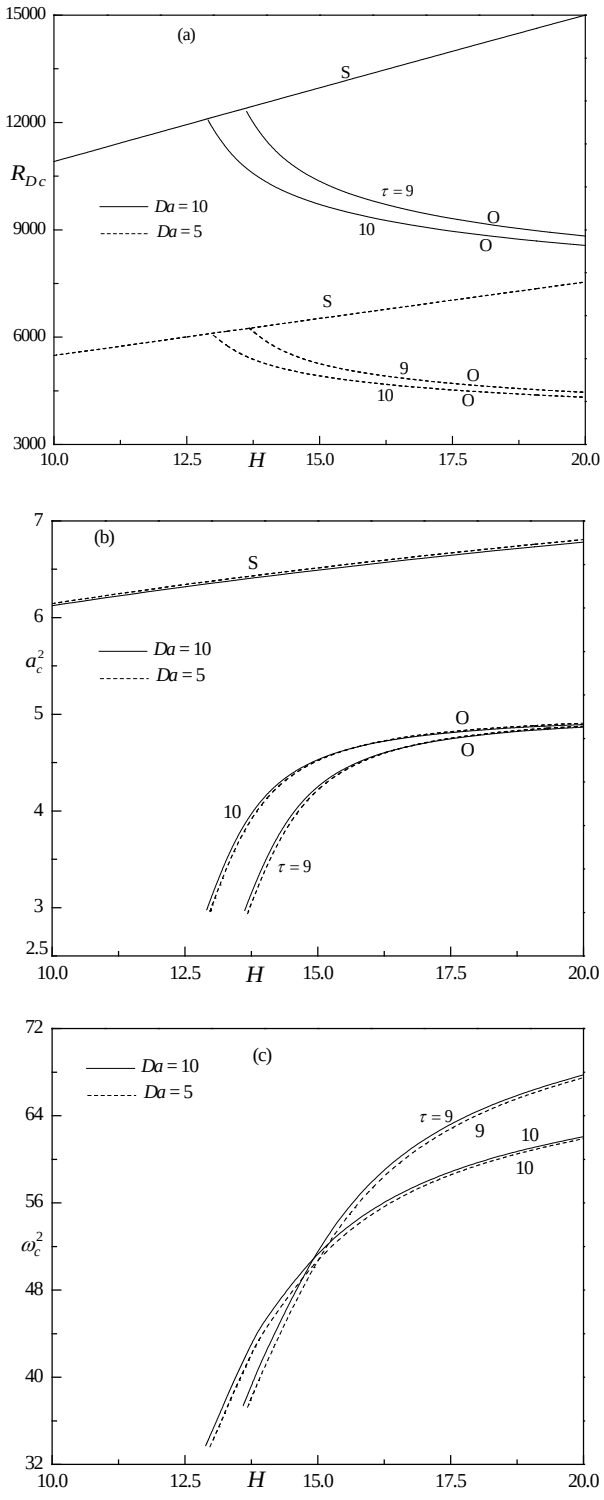

Fig. 7. Variation of **(a)** R_{Dc}, **(b)** a_c^2 : stationary (s), oscillatory(o), **(c)** ω_c^2 with H for Al_2O_3 solid skeleton when $Pr_D = 20$.

α	γ	Pr_D	R_{Dc}^O	a_c^2	ω_c^2	H^T
8.664×10^{-4} (CuO)	6.403×10^{-4} (CuO)	5	15956.1	3.56	2161.06	369.337
		10	10788.1	2.96	3004.69	242.315
		20	8584.5	2.80	3564.58	188.504
		∞	6779.4	2.90	4309.1	144.595
1.42×10^{-2} (Al_2O_3)	7.337×10^{-3} (Al_2O_3)	5	3279.9	2.88	241.67	61.479
		10	2862.5	2.82	278.90	51.094
		20	2670.5	2.83	299.54	46.356
		∞	2491.2	2.89	322.07	41.952
1	1	5	909.6	5.28	0.02996	6.395
		10	899.1	5.25	0.04013	5.943
		20	893.7	5.53	0.04631	5.718
		∞	888.2	5.22	0.05381	5.495

Table 1 The transition points H^T and the corresponding critical values of R_{Dc}^O, a_c^2 and ω_c^2 for different values of Darcy-Prandtl number when $Da = 1$ and $\tau = 1$.

α	γ	τ	R_{Dc}^{O}	a_c^2	ω_c^2	H^T
8.664×10^{-4} (CuO)	6.403×10^{-4} (CuO)	0.5	91542.6	2.79	8155.86	212.833
		1	66106.7	2.78	4144.36	148.093
		2	48510.8	2.80	2089.03	103.541
		3	40810.2	2.81	1395.12	84.123
		5	33137.7	2.83	836.68	64.845
		8	27641.0	2.86	521.49	51.093
		10	25454.4	2.87	416.35	45.641
1.42×10^{-2} (Al_2O_3)	7.337×10^{-3} (Al_2O_3)	0.5	31152.7	2.84	601.53	61.247
		1	23817.3	2.79	315.31	42.242
		2	18752.1	2.79	162.59	29.364
		3	16535.1	2.81	109.78	23.807
		5	14323.5	2.85	66.67	18.323
		8	12735.7	2.91	42.01	14.429
		10	12103.0	2.94	33.71	12.889
1	1	0.5	9221.4	5.36	0.0029	9.745
		1	8394.2	5.07	0.0491	5.503
		2	7852.0	4.89	0.0702	3.429
		3	7619.2	4.81	0.0706	2.664
		5	7390.4	4.74	0.0587	1.969
		8	7227.2	4.70	0.0467	1.508
		10	7162.5	4.69	0.0411	1.333

Table 2 The transition points H^T and the corresponding critical values of R_{Dc}^{O}, a_c^2 and ω_c^2 for different values of solid thermal relaxation time parameter when $Da = 10$ and $Pr_D = 20$.